

Hamiltonian Active Matter in Incompressible Fluid Membranes

Sneha Krishnan¹ and Rickmoy Samanta¹

¹*Birla Institute of Technology and Science, Pilani, Hyderabad Campus, Telangana 500078, India*
(Dated: December 11, 2025)

Active proteins and membrane-bound motors exert force dipole flows along fluid interfaces and lipid bilayers. We develop a unified hydrodynamic and Hamiltonian framework for the interactions of pusher and puller dipoles embedded in an *incompressible* two-dimensional membrane supported by a shallow viscous subphase. Beginning from the screened Stokes equations of the membrane-subphase composite, we derive the real-space incompressible Green's tensor, obtain its near- and far-field asymptotics, and construct the resulting dipolar velocity and stream functions. Although generic dipoles reorient under the local membrane vorticity, we show that the far-field dipolar flow is vorticity-free; force-free motors therefore retain fixed orientation and obey a Hamiltonian dynamics in which the positions of N dipoles evolve via an effective Hamiltonian built from the dipolar stream function. In the near field, where the flow possesses finite vorticity, a Hamiltonian formulation is recovered in the quenched-orientation limit. Exploiting this structure, we simulate ensembles of pusher and puller dipoles and compare the dynamics generated by the $1/r$ near-field kernel and the subphase screened $1/r^3$ far-field kernel. For identical dipoles, the far-field Hamiltonian produces rapid clustering from random initial conditions, whereas the near-field Hamiltonian suppresses collapse and yields extended, non-aggregating configurations.

I. INTRODUCTION

Active proteins, enzymes, and membrane-bound motors continually inject stress into biological interfaces, driving flows along fluid membranes and lipid bilayers. At the micron scale, inertia is negligible and these inclusions generate Stokesian flow fields whose leading contribution is a force dipole (stresslet) rather than a monopole [1, 2]. Such dipoles—extensile “pushers” and contractile “pullers”—play central roles in pattern formation, instabilities, and collective behaviour across active fluids [3–5]. Membrane-bound proteins and enzymatic assemblies act as force dipoles in vivo [6–8], and experiments have demonstrated motor-mediated clustering, cooperative pulling, and tension generation in reconstituted membranes [9, 10]. When these dipoles are confined to a two-dimensional interface, their hydrodynamic couplings differ sharply from those in bulk fluids, owing to the effectively planar geometry and momentum leakage into the surrounding three-dimensional subphase.

Supported membranes provide a particularly interesting setting in which these hydrodynamic effects have been worked out in detail. Classical analyses of membrane drag by Saffman, Delbrück, and their successors [11–17] showed that flows in a viscous membrane coupled to a finite-depth subphase obey a screened Stokes equation. The resulting Green's function exhibits two qualitatively distinct regimes: (i) a logarithmic “near field” with unscreened in-plane hydrodynamics producing $1/r$ dipolar flows, and (ii) a “far field” in which substrate friction produces algebraically screened $1/r^3$ flows. Recent studies of swimmers and active inclusions in thin films and membranes [18–21] highlight the richness of these interactions, but a systematic comparison of near- and far-field dipolar dynamics in supported membranes has been lacking.

In this work we develop a unified hydrodynamic and

Hamiltonian description of pusher and puller interactions in an *incompressible* supported membrane. Beginning from the screened Stokes equations of the membrane-subphase composite, we obtain the real-space Green's tensor, derive its near- and far-field asymptotics, and construct the associated dipolar velocity and stream functions. Although a generic dipole reorients in response to the local membrane vorticity, we show that the far-field dipolar flow is *vorticity free*. Force-free motors therefore maintain fixed orientation and admit a reduced Hamiltonian description closely related to recent two-dimensional Hamiltonian formulations of active particles [22]. In the near field, where vorticity is finite, a Hamiltonian structure is recovered in the quenched-orientation limit.

Exploiting this framework, we compare the collective behaviour generated by the unscreened and screened kernels for ensembles of identical pushers and pullers. The contrast is striking: the far-field Hamiltonian produces rapid collapse into compact clusters, whereas the near-field Hamiltonian suppresses aggregation and yields extended, non-collapsing configurations. These trends persist across a wide range of initial geometries and motor types, demonstrating that the structure of the hydrodynamic kernel—not the sign of the dipole alone—determines whether a membrane-bound active ensemble aggregates or disperses.

Taken together, our results show that even in the simplest incompressible limit, the hydrodynamic screening intrinsic to supported membranes imposes strong, kernel-dependent constraints on collective organisation. This work provides a foundation for Hamiltonian approaches to active matter on interfaces and sets the stage for extensions to chiral membranes, curved geometries, and biologically driven active films [20, 21, 23, 24].

II. INCOMPRESSIBLE SUPPORTED MEMBRANE

We consider a two-dimensional viscous membrane of shear viscosity η_s lying in the plane $z = h$, supported by a Newtonian subphase of viscosity η and thickness h above a rigid wall (Fig. 1). Throughout the main text we restrict to the incompressible limit: the in-plane velocity field $\mathbf{v}(\mathbf{r})$ satisfies $\nabla \cdot \mathbf{v} = 0$, there is no dilatational viscosity.

Eliminating the three-dimensional subphase flow under a lubrication approximation yields an effective Brinkman friction acting on the membrane [16, 23], so that the steady Stokes balance reads

$$\eta_s \nabla^2 \mathbf{v} - \frac{h}{2} \nabla p - \zeta_{\parallel} \mathbf{v} + \mathbf{F} = \mathbf{0}, \quad \nabla \cdot \mathbf{v} = 0, \quad (1)$$

where p is the membrane pressure, $\mathbf{F}(\mathbf{r})$ is any in-plane body force density, and ζ_{\parallel} is a phenomenological friction coefficient that encodes momentum leakage into the subphase. For a shallow film one typically expects

$$\zeta_{\parallel} \sim \frac{\eta}{h},$$

so that the hydrodynamic screening length

$$\kappa^{-1} = \sqrt{\frac{\eta_s}{\zeta_{\parallel}}} = \sqrt{\frac{\eta_s h}{\eta}}$$

sets the crossover between “membrane-dominated” and “subphase-dominated” flow.

Because Eq. (1) is linear and translationally invariant in the membrane plane, the velocity response to a localized in-plane force $\mathbf{F}(\mathbf{r}) = \mathbf{f} \delta(\mathbf{r})$ can be written in terms of a Green’s tensor $G_{ij}(\mathbf{r})$,

$$v_i(\mathbf{r}) = G_{ij}(\mathbf{r}) f_j.$$

In Fourier space, incompressibility projects onto transverse components, and the Brinkman operator becomes

$$\tilde{G}_{ij}(\mathbf{q}) = \frac{1}{\eta_s(q^2 + \kappa^2)} (\delta_{ij} - \hat{q}_i \hat{q}_j), \quad (2)$$

where $\hat{\mathbf{q}} = \mathbf{q}/q$. The real-space Green’s tensor is obtained from the inverse transform

$$G_{ij}(\mathbf{r}) = \int \frac{d^2 q}{(2\pi)^2} e^{i\mathbf{q} \cdot \mathbf{r}} \tilde{G}_{ij}(\mathbf{q}).$$

Rotational invariance implies the decomposition

$$G_{ij}(\mathbf{r}) = \frac{1}{2\pi\eta_s} \left[A(r) \delta_{ij} + B(r) \hat{r}_i \hat{r}_j \right], \quad (3)$$

with $r = |\mathbf{r}|$ and $\hat{\mathbf{r}} = \mathbf{r}/r$. Explicit integration yields

$$A(r) = K_0(\kappa r) + \frac{K_1(\kappa r)}{\kappa r} - \frac{1}{\kappa^2 r^2}, \quad (4)$$

$$B(r) = -K_0(\kappa r) - \frac{2K_1(\kappa r)}{\kappa r} + \frac{2}{\kappa^2 r^2}, \quad (5)$$

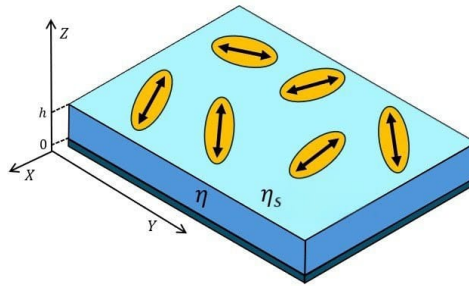


FIG. 1: Schematic of active force-dipole motors confined to a supported fluid membrane. Orange ellipses denote motors with orientations (double arrows). The light blue layer is an incompressible two-dimensional membrane of shear viscosity η_s , supported by a viscous subphase of viscosity η and thickness h above a rigid wall.

where K_n are modified Bessel functions of the second kind. Equations (3)–(5) constitute the screened two-dimensional Stokeslet for an incompressible supported membrane [16, 17].

III. DIPOLAR FLOWS: NEAR AND FAR ZONES

Force-free active inclusions such as membrane-anchored motors are naturally modelled as force dipoles (stresslets). A point stresslet of strength σ and orientation $\hat{\mathbf{d}}$ located at the origin can be represented as the derivative of the Stokeslet along the dipole axis,

$$v_i(\mathbf{r}) = \sigma \hat{d}_k \partial_k G_{ij}(\mathbf{r}) \hat{d}_j, \quad (6)$$

with $\hat{\mathbf{d}} = (\cos \alpha, \sin \alpha)$. Introducing polar coordinates (r, θ) for \mathbf{r} , we can express the velocity in terms of radial and azimuthal components v_r and v_θ .

A. Near field: unscreened logarithmic hydrodynamics

For separations much smaller than the screening length, $\kappa r \ll 1$, the Bessel functions admit the expansions

$$A(r) \simeq \frac{1}{4} \left[-1 - 2\gamma - 2 \ln \left(\frac{\kappa r}{2} \right) \right], \quad (7)$$

$$B(r) \simeq \frac{1}{2},$$

where γ is Euler’s constant. Substituting these into Eq. (6) and differentiating yields a purely radial near-field flow for a dipole placed at the origin, with the orientation angle α ,

$$\mathbf{v}_{\text{near}}(\mathbf{r}) = \frac{\sigma}{4\pi\eta_s r} \cos[2(\alpha - \theta)] \hat{\mathbf{r}}, \quad (\kappa r \ll 1), \quad (8)$$

characteristic of a two-dimensional stresslet with logarithmic hydrodynamics.

An incompressible two-dimensional flow may be written in terms of a scalar stream function $\Psi(r, \theta)$ via

$$v_r = \frac{1}{r} \partial_\theta \Psi, \quad v_\theta = -\partial_r \Psi. \quad (9)$$

For Eq. (8) one finds

$$\Psi_{\text{near}}(r, \theta) = -\frac{\sigma}{8\pi\eta_s} \sin[2(\alpha - \theta)], \quad (10)$$

and the scalar vorticity,

$$\omega_z^{(\text{near})}(r, \theta) = -\frac{\sigma}{2\pi\eta_s r^2} \sin[2(\alpha - \theta)], \quad (11)$$

is nonzero except along the principal axes, indicating that the near-field flow is locally vortical.

B. Far field: algebraically screened potential flow

At distances much larger than the screening length, $\kappa r \gg 1$, the exponential decay of $K_n(\kappa r)$ leaves only the algebraic terms in Eqs. (4)–(5),

$$A(r) \simeq -\frac{1}{\kappa^2 r^2}, \quad B(r) \simeq \frac{2}{\kappa^2 r^2}.$$

Substituting into Eq. (6) gives the far-field velocity

$$\mathbf{v}_{\text{far}}(\mathbf{r}) = \frac{\sigma}{\pi\zeta_{\parallel} r^3} \left[\cos(2\Delta) \hat{\mathbf{r}} - \sin(2\Delta) \hat{\boldsymbol{\theta}} \right], \quad (\kappa r \gg 1), \quad (12)$$

where $\Delta = \alpha - \theta$ and we have used $\kappa^2 = \zeta_{\parallel}/\eta_s$. The flow now decays as r^{-3} and has both radial and azimuthal components.

Using the stream-function representation, one finds

$$\Psi_{\text{far}}(r, \theta) = -\frac{\sigma}{2\pi\zeta_{\parallel}} \frac{\sin[2(\alpha - \theta)]}{r^2}, \quad (13)$$

which smoothly matches the near-field expression at $r \sim \kappa^{-1}$. In contrast to the near zone, the far-field flow is irrotational away from the dipole singularity:

$$\omega_z^{(\text{far})}(r, \theta) = 0 \quad (r > 0). \quad (14)$$

IV. HAMILTONIAN FORMULATION FOR DIPOLES

The *incompressible* membrane enjoys a useful structural simplification: for force dipoles with *fixed* orientations, the positional dynamics can be written in Hamiltonian form. Let the position of dipole i be $\mathbf{r}_i = (x_i, y_i)$, with strength $\sigma_i = \pm 1$ (pusher or puller) and fixed orientation angle α_i . The velocity of dipole i is obtained by

evaluating the dipolar flow generated by all other dipoles $j \neq i$ at \mathbf{r}_i :

$$\dot{\mathbf{r}}_i = \sum_{j \neq i} \mathbf{v}_j(\mathbf{r}_i - \mathbf{r}_j).$$

Using the stream function representation, this can be recast as

$$\sigma_i \dot{\mathbf{r}}_i = \hat{\mathbf{z}} \times \nabla_i H, \quad H = \sum_{i \neq j} \sigma_i \Psi_j(\mathbf{r}_{ij}), \quad (15)$$

where $\mathbf{r}_{ij} = \mathbf{r}_i - \mathbf{r}_j$ and Ψ_j is the stream function generated by dipole j (near or far, depending on the regime of interest). Equation (15) shows that (x_i, y_i) play the role of canonical variables with an effective Hamiltonian determined by the hydrodynamic kernel.

A. Near-field Hamiltonian

As noted in Eq. (11), the unscreened near-field dipolar flow carries finite vorticity, so freely rotating dipoles undergo hydrodynamic reorientation. These orientational dynamics preclude a Hamiltonian written solely in terms of particle positions. A reduced Hamiltonian description is nevertheless recovered in the *quenched-orientation* limit, where dipole axes are externally constrained or relax much faster than translational motion. This regime is natural for anchored “shakers” and for strongly aligned active suspensions [3–5, 22]. With orientations fixed, the near-field stresslet retains its $1/r$ form and generates a consistent position-based Hamiltonian, enabling a direct comparison with the far-field dynamics. Thus, in the unscreened regime ($\kappa r_{ij} \ll 1$), the stream function of dipole j is given by Eq. (10),

$$\Psi_j^{(\text{near})} = \frac{\sigma_j}{8\pi\eta_s} \sin[2(\theta_{ij} - \alpha_j)],$$

leading to the Hamiltonian

$$H_{\text{near}} = \frac{1}{8\pi\eta_s} \sum_{i \neq j} \sigma_i \sigma_j \sin[2(\theta_{ij} - \alpha_j)]. \quad (16)$$

For co-aligned dipoles ($\alpha_j = \alpha$), a global rotation sets $\alpha = 0$, simplifying the angular structure. Differentiating Eq. (16) then yields explicit equations of motion that generate the $1/r$ near-field stresslet flows.

B. Far-field Hamiltonian

In the screened regime ($\kappa r \gg 1$), the dipolar flow becomes *vorticity free*, as shown in Eq. (14). With no hydrodynamic torque acting on the dipole axes, orientations remain fixed and the dynamics reduce naturally to a position-only description. This irrotational structure, together with membrane incompressibility, makes the far

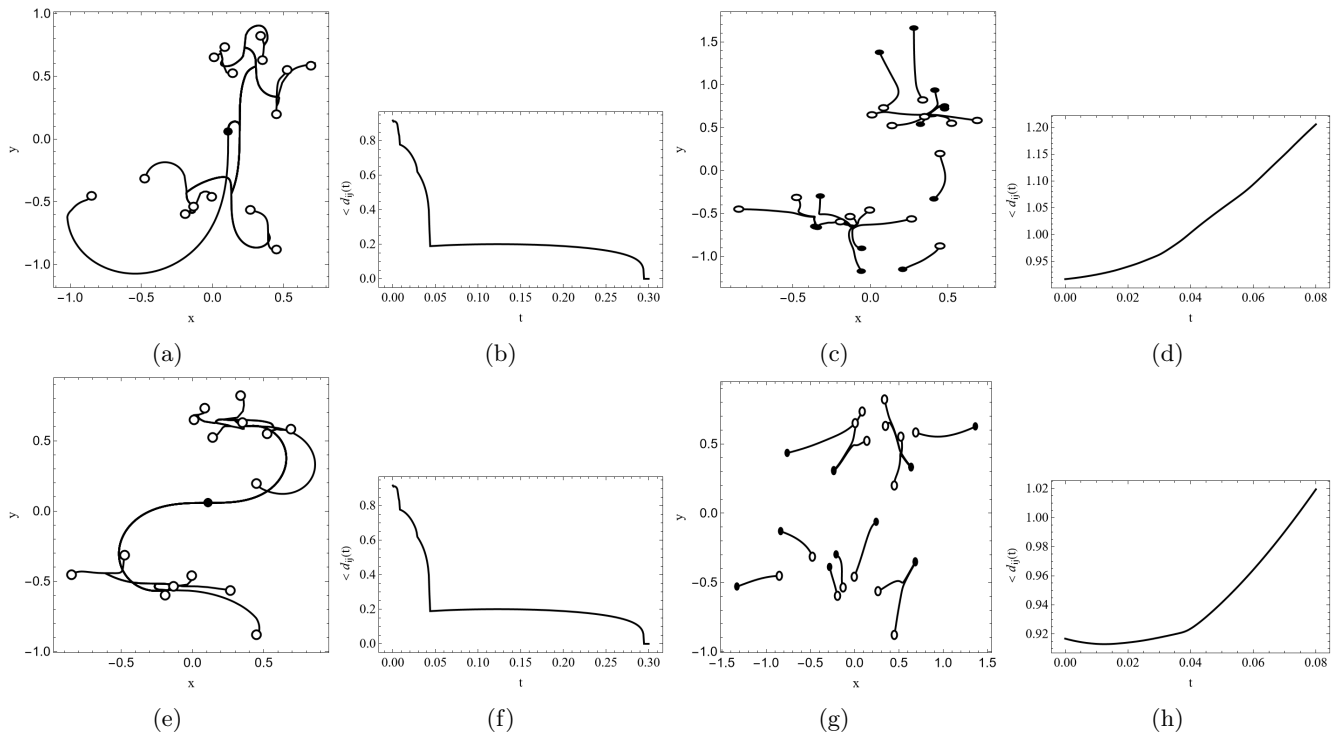


FIG. 2: Dynamics of $N = 15$ pusher (top row) and puller (bottom row) dipoles in an incompressible supported membrane. Open circles mark initial positions; filled black dots mark final positions. (a–b,e–f) Evolution under the screened far-field Hamiltonian H_{far} : particle trajectories (a,e) and mean pair separation $\langle d_{ij}(t) \rangle$ (b,f). Both pushers and pullers exhibit strong mutual attraction and collapse into compact clusters. (c–d,g–h) Evolution under the unscreened near-field Hamiltonian H_{near} in the quenched-orientation limit: trajectories (c,g) and $\langle d_{ij}(t) \rangle$ (d,h). In both cases the ensembles expand and $\langle d_{ij}(t) \rangle$ grows monotonically, demonstrating that near-field interactions suppress the far-field aggregation instability.

field an *intrinsically* Hamiltonian regime: the pairwise interactions derive directly from the screened stream function. For well-separated dipoles ($\kappa r_{ij} \gg 1$), the screened stream function (13) yields

$$H_{\text{far}} = \frac{1}{2\pi\zeta_{\parallel}} \sum_{i \neq j} \frac{\sigma_i \sigma_j}{r_{ij}^2} \sin[2(\theta_{ij} - \alpha_j)], \quad (17)$$

The associated equations of motion,

$$\dot{x}_i = \frac{1}{\sigma_i} \frac{\partial H}{\partial y_i}, \quad \dot{y}_i = -\frac{1}{\sigma_i} \frac{\partial H}{\partial x_i}, \quad (18)$$

generate the $1/r^3$ screened flows of Eq. (12). For co-aligned dipoles, both Hamiltonians reduce to simple functions of the relative polar angles, $H \propto \sum_{i \neq j} \sigma_i \sigma_j \sin(2\theta_{ij})/r_{ij}^n$ with $n = 0$ or 2 .

V. COLLECTIVE DYNAMICS OF PUSHER AND PULLER DIPOLES

We probe the dynamical consequences of the two kernels by separately simulating ensembles of identical pushers and pullers ($\sigma_i = \pm 1$) with fixed, co-aligned orientations. In the far field, the flow is vorticity-free and

orientations are naturally quenched, making H_{far} an exact position-based Hamiltonian. In the near field, where vorticity is finite, a Hamiltonian description applies only in the enforced quenched-orientation limit. Within these regimes, we contrast the collective organization produced by H_{far} and H_{near} .

A. Simulation details

We integrate the $2N$ position variables $\{x_i(t), y_i(t)\}$ using a standard adaptive Runge-Kutta method, evolving Eq. (18) with either H_{near} or H_{far} . Throughout this section we take $N = 15$ and use identical random initial positions for both kernels: particles are sampled uniformly from a unit disc. Initial positions are indicated by open circles in Fig. 2, while filled black circles mark the final positions at $t = t_{\text{max}}$. To quantify aggregation or dispersion, we monitor the mean pairwise separation

$$\langle d_{ij}(t) \rangle = \frac{2}{N(N-1)} \sum_{i < j} \sqrt{\Delta x_{ij}^2 + \Delta y_{ij}^2}, \quad (19)$$

where $\Delta x_{ij} = x_i - x_j$ and $\Delta y_{ij} = y_i - y_j$. A small softening parameter ϵ was added inside the squared dis-

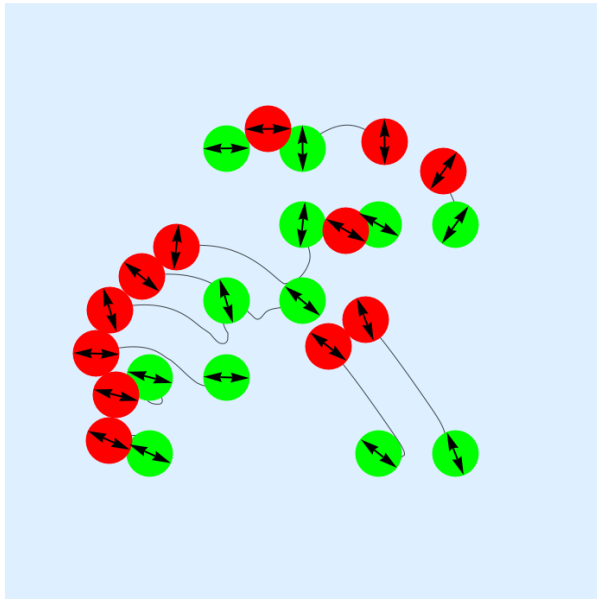


FIG. 3: Representative far-zone dynamics of a randomly initialized cluster of twelve pushers in the incompressible membrane with *random* initial locations (within a disc) and *random* orientations. Green disks indicate initial positions, red disks indicate final positions, and the grey curves trace the particle trajectories. A soft harmonic repulsion is included to regularize close encounters.

tance to regularize close encounters without altering the large-scale flow. Energy conservation, $\dot{H} = 0$ (between collisions) is verified to within a relative tolerance of 10^{-6} , confirming numerical accuracy.

B. Near vs. far: aggregation and dispersion

The collective dynamics of active dipoles in an incompressible membrane depend crucially on whether interactions are mediated by the algebraically screened far-field kernel or by the unscreened near-field kernel. Figure 2 summarizes the behaviour for ensembles of $N = 15$ *pushers* (top row) and *pullers* (bottom row).

Under the screened far-field Hamiltonian H_{far} [Figs. 2(a,b,e,f)], both motor types undergo a rapid collapse into compact aggregates: trajectories contract toward a single point and the mean pair separation $\langle d_{ij} \rangle(t)$ decreases sharply before saturating at a small value. This aggregation reflects the effectively attractive character of the $1/r^3$ screened dipolar flow, which reinforces head-to-tail alignment and produces a robust self-binding instability for both pushers and pullers.

In contrast, evolution under the unscreened near-field Hamiltonian H_{near} [Figs. 2(c,d,g,h)] exhibits a completely different trend. The $1/r$ stresslet decay is slower and we find that the ensemble does not collapse. Instead, par-

ticles spread into extended configurations and $\langle d_{ij} \rangle(t)$ grows monotonically. In this near-zone regime, the self-aggregation observed in the far field is vastly suppressed: although individual pairs can transiently attract or repel, many-body constraints prevent the formation of a stable compact cluster.

The similarity between the pusher and puller panels highlights a central result of this work: *the nature of the hydrodynamic kernel, rather than the motor type alone, determines whether active dipoles aggregate or disperse*. The far-field screened flow is irrotational and generates an attractive effective Hamiltonian, while the near-field unscreened flow frustrates collective collapse. For completeness, Fig. 3 shows a representative far-zone evolution with *arbitrary* orientations, illustrating that the same aggregation mechanism persists beyond the co-aligned limit. Representative far- and near-zone trajectories of co-aligned pusher and puller clusters are provided in the Supplementary Material (Figs. S1–S2). In all these examples, a soft harmonic repulsion is added to regularize close encounters and suppress particle overlap.

VI. SUMMARY AND OUTLOOK

We have developed a minimal hydrodynamic Hamiltonian framework for active force dipoles confined to an *incompressible* supported membrane. Starting from the Brinkman-regularized Stokes equation, we derived the screened incompressible Green's tensor, identified its logarithmic near-field and algebraically screened far-field limits, and constructed the associated dipolar flows and stream functions. A key outcome of this analysis is the emergence of two distinct Hamiltonian regimes. In the far field, the screened flow is strictly vorticity-free, so dipole orientations remain naturally quenched; membrane incompressibility then yields an *exact* position-based Hamiltonian H_{far} . In contrast, the near field possesses finite vorticity, precluding an orientation-dynamics-free description; a Hamiltonian formulation applies only in the *enforced* quenched-orientation limit, defining the effective Hamiltonian H_{near} . Within these regimes, we contrasted the collective organization generated by the two kernels.

This comparison reveals a striking dichotomy. For identical pushers (and similarly for pullers), the algebraically screened $1/r^3$ far-field interactions produce a strong self-binding instability, driving rapid collapse into compact clusters and a sharp decay of the mean pair separation. The unscreened $1/r$ near-field kernel behaves qualitatively differently: it induces strong local rearrangements but no long-lived aggregates, and the ensemble disperses monotonically in time, rendering near-zone dynamics intrinsically non-aggregating. This contrast persists across motor types and initial orientations, showing that it is the *hydrodynamic kernel*—not merely the dipole sign—that controls collective organization. These results offer a controlled framework for

interpreting more complex membrane rheologies. Allowing membrane compressibility opens a longitudinal mobility channel that breaks the Hamiltonian structure and can enhance aggregation for pullers [24] while producing mixed responses for pushers. Introducing odd (Hall) viscosity adds antisymmetric stresses that drive chiral transport and circulating cluster states [24]. Coupling the membrane to curvature, shape fluctuations, or biochemical activity further broadens the phenomenology, enabling a range of richer and biologically relevant collective behaviours. More broadly, the incompressible supported membrane studied here provides a simple yet dynamically rich framework for future works on compressible, chiral, or curved membranes, and it motivates experimental tests in reconstituted active films where the screening length and membrane viscosities can be precisely tuned. The Hamiltonian formulation developed in this work offers a minimal yet powerful analytical framework for probing active matter at interfaces, and highlights the central role of hydrodynamic screening in shaping collective organization.

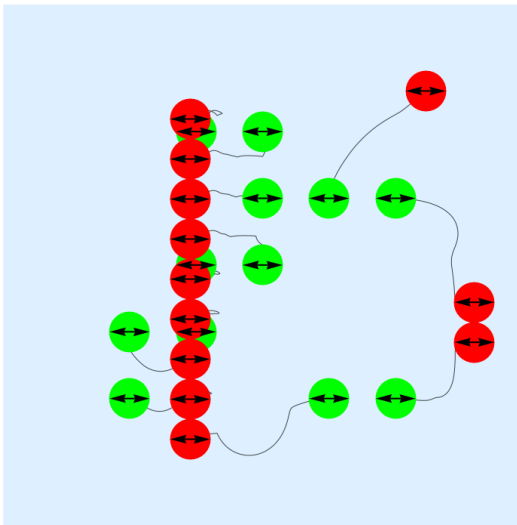
ACKNOWLEDGMENTS

We are very thankful to Sarthak Bagaria, Naomi Oppenheimer, Haim Diamant, Michael D. Graham, and Mark Henle. S.K. acknowledges support from an Institute fellowship at Birla Institute of Technology and Science, Pilani (Hyderabad Campus). R.S. is supported by a DST INSPIRE Faculty fellowship, India (Grant No. IFA19-PH231), NFSG, and an OPERA Research Grant from Birla Institute of Technology and Science, Pilani (Hyderabad Campus).

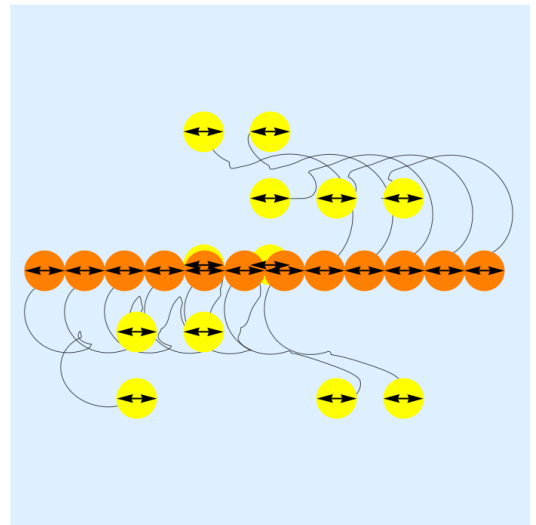
DATA AVAILABILITY

The data that support the findings of this study are available within the article.

-
- [1] E. M. Purcell, *Life at low Reynolds number*, Am. J. Phys. **45**, 3 (1977).
- [2] E. Lauga and T. R. Powers, *The hydrodynamics of swimming microorganisms*, Rep. Prog. Phys. **72**, 096601 (2009).
- [3] Y. Hatwalne, S. Ramaswamy, M. Rao, and R. A. Simha, *Rheology of active-particle suspensions*, Phys. Rev. Lett. **92**, 118101 (2004).
- [4] T. Vicsek, A. Czirók, E. Ben-Jacob, I. Cohen, and O. Shochet, *Novel type of phase transition in a system of self-driven particles*, Phys. Rev. Lett. **75**, 1226 (1995).
- [5] M. C. Marchetti, J.-F. Joanny, S. Ramaswamy, T. B. Liverpool, J. Prost, M. Rao, and R. A. Simha, *Hydrodynamics of soft active matter*, Rev. Mod. Phys. **85**, 1143 (2013).
- [6] N. S. Gov and S. A. Safran, *Red blood cell membrane fluctuations and shape controlled by ATP-induced cytoskeletal defects*, Biophys. J. **88**, 1859 (2005).
- [7] B. A. Camley and F. L. H. Brown, *Diffusion of complex objects embedded in free and supported lipid bilayer membranes: role of shape and hydrodynamic coupling*, Soft Matter **9**, 4767 (2013).
- [8] A. S. Mikhailov and R. Kapral, *Hydrodynamic collective effects of active protein machines in solution and lipid bilayers*, Proc. Natl. Acad. Sci. USA **112**, E3639 (2015).
- [9] O. Campàs, C. Leduc, P. Bassereau, J. Casademunt, J.-F. Joanny, and J. Prost, *Coordination of kinesin motors pulling on fluid membranes*, Biophys. J. **94**, 5009 (2008).
- [10] R. Grover, J. Fischer, F. W. Schwarz, W. J. Walter, P. Schwille, and S. Diez, *Transport efficiency of membrane-anchored kinesin motors depends on motor density and diffusivity*, Proc. Natl. Acad. Sci. USA **113**, E7185 (2016).
- [11] P. G. Saffman, *Brownian motion in thin sheets of viscous fluid*, J. Fluid Mech. **73**, 593 (1975).
- [12] P. G. Saffman and M. Delbrück, *Brownian motion in biological membranes*, Proc. Natl. Acad. Sci. USA **72**, 3111 (1975).
- [13] B. D. Hughes, B. A. Pailthorpe, and L. R. White, *The translational and rotational drag on a cylinder moving in a membrane*, J. Fluid Mech. **110**, 349 (1981).
- [14] E. Evans and E. Sackmann, *Translational and rotational drag coefficients for a disk in a supported liquid membrane*, J. Fluid Mech. **194**, 553 (1988).
- [15] D. K. Lubensky and R. E. Goldstein, *Hydrodynamics of monolayer domains at the air-water interface*, Phys. Fluids **8**, 843 (1996).
- [16] H. A. Stone and A. Ajdari, *Hydrodynamics of particles embedded in a surfactant layer over a subphase of finite depth*, J. Fluid Mech. **369**, 151 (1998).
- [17] T. M. Fischer, *The drag on needles moving in a Langmuir monolayer*, J. Fluid Mech. **498**, 123 (2004).
- [18] M. Leoni and T. B. Liverpool, *Swimmers in thin films: from swarming to hydrodynamic instabilities*, Phys. Rev. Lett. **105**, 238102 (2010).
- [19] H. Manikantan, *Tunable collective dynamics of active inclusions in viscous membranes*, Phys. Rev. Lett. **125**, 268101 (2020).
- [20] S. Bagaria and R. Samanta, *Dynamics of force dipoles in curved fluid membranes*, Phys. Rev. Fluids **7**, 093101 (2022).
- [21] S. Jain and R. Samanta, *Force dipole interactions in tubular fluid membranes*, Phys. Fluids **35**, 071901 (2023).
- [22] Y. Shoham and N. Oppenheimer, *Hamiltonian dynamics and structural states of two-dimensional active particles*, Phys. Rev. Lett. **131**, 178301 (2023).
- [23] Y. Hosaka, D. Andelman, and S. Komura, "Pair dynamics of active force dipoles in an odd-viscous fluid," *Eur. Phys. J. E* **46**, 18 (2023).
- [24] S. Krishnan, U. Maurya, and R. Samanta, in preparation (2025).

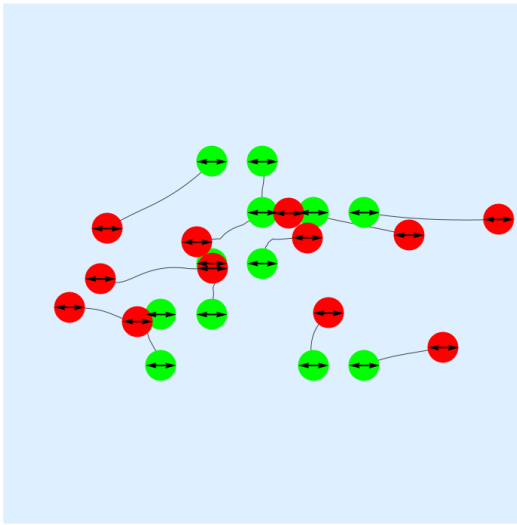


(a) Pushers.

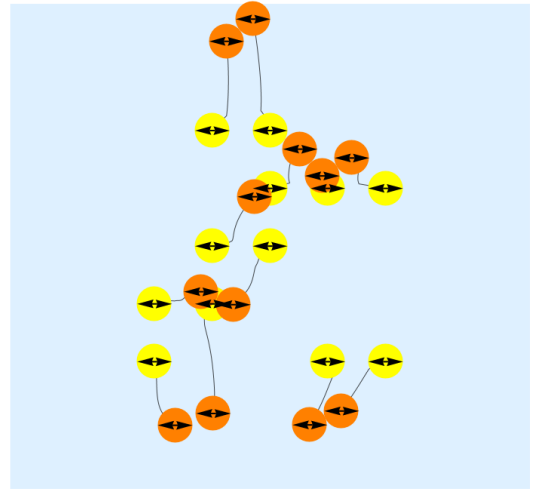


(b) Pullers.

FIG. S1: Far-zone dynamics of co-aligned clusters of twelve pushers (left) and pullers (right) in an incompressible membrane, initialized at random locations within a disc. Initial positions appear in green (pushers) and yellow (pullers), final positions in red and orange, with trajectories in grey. A soft harmonic repulsion is included to prevent particle overlap.



(a) Pushers.



(b) Pullers.

FIG. S2: Representative near-zone dynamics of randomly initialized (within a disc), co-aligned clusters of twelve pushers (left) and pullers (right) in an incompressible membrane. Initial positions are shown in green (pushers) and yellow (pullers); final positions in red and orange, respectively; trajectories are grey. A soft harmonic repulsion is included to regularize close encounters.

Supplemental Material for
“Hamiltonian Active Matter in Incompressible Fluid Membranes”